JOURNAL OF SPACECRAFT AND ROCKETS
Vol. 41, No. 6, November–December 2004

Rotating Formation Flying of Three Satellites Using Tethers

K. D. Kumar* and T. Yasaka†
Kyushu University, Fukuoka 812-8581, Japan

The feasibility of rotating formation flying of satellites using flexible tethers is explored. The system is composed of three satellites connected through tethers and located at the vertices of a triangle-like configuration. The satellites are modeled as point masses, and tethers are considered massless. The general formulation of the governing equations of motions of the system moving in an elliptic orbit and including different satellite masses and tether lengths is obtained through a Lagrangian approach. The open-loop tether deployment and retrieval laws have been developed. Results of numerical simulations of the nonlinear governing equations of motion of the proposed constrained system and an equilibrium analysis indicate the feasibility of achieving formation flying of three satellites in the orbital plane. Furthermore, the equilibrium analysis leads to useful design criteria in the form of inequality constraints on the system parameters. In the case when three satellites have equal masses, the critical minimum value of spin rate for system steady-spin motion in the orbital plane is found to be 0.58 times the orbital rate. Finally, the effects of various system parameters as well as the tether deployment and retrieval on the system response have been investigated.

Nomenclature

a	=	semimajor axis of the system center of mass, m
C	=	$EA/(m\Omega^2)$, m
Cj	=	$C\{(1-e^2)/(1+e\cos\theta)\}^3\varepsilon_j u_j$; $j=1, 2, 3$, m
C_t	=	$EA/(ml_{10}\Omega^2)$
$(C_t)_{\rm cr}$	=	critical or minimum C_t for system steady-spin motion
EA	=	tether modulus of rigidity, N
e	=	orbital eccentricity
f_i	=	ith constraint function
G	=	universal gravitational constant, $\mathrm{kg}^{-1}\mathrm{m}^{-2}$
l_j	=	stretched jth tether length; $j=1, 2, 3$, m
$l_{\rm je}$	=	stretched jth tether length at equilibrium; $j=1, 2, 3$, m
l_{j0}	=	unstretched jth tether length; $j=1, 2, 3$, m
$(l_{j0})_{\rm cr}$	=	critical or minimum unstretched jth tether length; $j=1, 2, 3$, m
$l_{j0,e}$	=	unstretched jth tether length at equilibrium; $j=1, 2, 3$, m
$l_{j0,f}$	=	final unstretched jth tether length at the end of deployment or retrieval; $j=1, 2, 3$, m
$l_{j0,i}$	=	initial unstretched jth tether length at the start of deployment or retrieval; $j=1, 2, 3$, m
l'_{j0}	=	rate of unstretched jth tether length change during deployment or retrieval; $j=1, 2, 3$
l_{t0}	=	l_{10} or l_{20} when $l_{10}=l_{20}$, m
M_E	=	Earth's mass, kg
m	=	system mass, $m_1+m_2+m_3$, kg
m_i	=	mass of satellite i; $i=1, 2, 3$, kg
R	=	orbital radius, m
r_i	=	distance between system mass center S and satellite i; $i=1, 2, 3$, m
$r_{\rm ie}$	=	r_i at system equilibrium; $i=1, 2, 3$, m
r_{i0}	=	r_i at $\theta=0$; $i=1, 2, 3$, m
r'_{i0}	=	r'_i at $\theta=0$; $i=1, 2, 3$
S	=	system mass center
$S-x_{\rm ri}y_{\rm ri}z_{\rm ri}$	=	coordinate frame describing $\boldsymbol{r}_i$; $i=1, 2, 3$
$S-x_0y_0z_0$	=	coordinate axes in the local vertical frame
T	=	kinetic energy of the system, N-m
u_j	=	unit function, 1 for $\varepsilon_j\geq 0$ and 0 for $\varepsilon_j<0$; $j=1, 2, 3$
V	=	potential energy of the system, N-m
β'_e	=	β'_{1e} or β'_{2e} when $\beta'_{1e}=\beta'_{2e}$
β_i	=	in-plane swing angle of $\boldsymbol{r}_i$; $i=1, 2, 3$, deg
$\beta_{\rm ie}$	=	β_i at system equilibrium; $i=1, 2, 3$, deg
$\beta'_{\rm ie}$	=	β'_i at system equilibrium; $i=1, 2, 3$
β_{i0}	=	β_i at $\theta=0$; $i=1, 2, 3$, deg
β'_{i0}	=	β'_i at $\theta=0$; $i=1, 2, 3$
β'_0	=	β'_{10} or β'_{20} when $\beta'_{10}=\beta'_{20}$
$(\beta'_0)_{\rm cr}$	=	critical or minimum β'_0 for system steady-spin motion
ε_j	=	jth tether strain; $j=1, 2, 3$
η_i	=	out-of-plane swing angle of $\boldsymbol{r}_i$; $i=1, 2, 3$, deg
$\eta_{\rm ie}$	=	η_i at system equilibrium; $i=1, 2, 3$, deg
$\eta'_{\rm ie}$	=	η'_i at system equilibrium; $i=1, 2, 3$
η_{i0}	=	η_i at $\theta=0$; $i=1, 2, 3$, deg
η'_{i0}	=	η'_i at $\theta=0$; $i=1, 2, 3$
η'_0	=	η'_{10} or η'_{20} when $\eta'_{10}=\eta'_{20}$
θ	=	true anomaly as measured from the reference line, deg
θ_{r0}	=	θ when deployment/retrieval starts, deg
Λ_i	=	Lagrange multiplier for ith constraint
λ_i	=	$[1/(m\Omega^2)][(1-e^2)/(1+e\cos\theta)]^3\Lambda_i$; $i=1, 2, 3$
μ_i	=	m_i/m; $i=1, 2, 3$
τ	=	number of orbits desired for completing the required tether deployment/retrieval
Ω	=	mean orbital angular velocity $(GM_E/a^3)^{1/2}$, rad/s
ω_c	=	angular velocity of circular orbit, rad/s
$()_{\rm cr}$	=	critical or minimum value of $()$
$()_j$	=	$()$ for jth tether, $j=1, 2, 3$
$()_0$	=	$()$ at $\theta=0$
$(\dot{})$, $(\ddot{})$	=	$\mathrm{d}()/\mathrm{d}t$ and $\mathrm{d}^2()/\mathrm{d}t^2$, respectively
$()'$, $()''$	=	$\mathrm{d}()/\mathrm{d}\theta$ and $\mathrm{d}^2()/\mathrm{d}\theta^2$, respectively
$\lvert()\rvert_{\max}$	=	absolute maximum amplitudes of $()$

Received 27 January 2003; revision received 21 July 2003; accepted for publication 20 November 2003.

*Japan Society for the Promotion of Science Fellow, Department of Aeronautics and Astronautics, 6-10-1 Hakozaki, Higashi-ku; krishnadevkumar@yahoo.com. Member AIAA.

†Professor, Department of Aeronautics and Astronautics; yasaka@aero.kyushu-u.ac.jp. Member AIAA.

Introduction

SATELLITE formation flying is one of the most important technologies for future space missions. However, it involves tremendous challenges ranging from satellite formation initialization to reconfiguration. The satellite formation flying can experience

environmental disturbances from gravitational perturbation, atmospheric drag, solar radiation pressure, and electromagnetic forces. Furthermore, as fuel onboard is a scarce commodity, it is necessary to have a formation with minimum fuel requirements for orbit maintenance. To solve these challenges, various strategies[1–9] have been suggested. The use of tethers[10–13] represents one of the important strategies to achieve satellite formation flying with low fuel requirements for overall system maintenance. Besides allowing the separation distance between the satellites to be well known and controllable, it can make a variable baseline for interferometric observations achievable by deploying or retrieving the tether. Tethered formation flying has been considered for astronomical observation missions[14–21] and Earth-observation missions.[19,22–24] DeCou[15–17] studied the dynamics of a rotating triangular formation of three tethered satellites with the spin rate of the formation being larger than the orbital rate for a geocentric astronomical observation mission. The spin axis of the formation was intended to remain inertially fixed. The proposal of the tethered Submillimeter Probe of the Evolution of Cosmic Structure mission flying at sun–Earth L_2 Lagrange point was put forward by Quinn and Folta.[18] Quadrelli[19] examined the heliocentric inertially pointed astronomical multitethered system configuration and librating tether in low Earth orbit (LEO) for synthetic aperture radar Earth observation. The formations applicable to deep-space astronomy have also been studied by Bomardelli et al.[20] and Misra et al.[21] Tragesser[22] undertook the same problem of rotating triangular formation of three tethered satellites that was earlier studied by DeCou[15–17] and considered two cases: the first case being the cylindrical case in which the plane of the formation is in the orbital plane and the second case termed the conical case in which the spin axis traces out a cone with the Earth at the center of the base of the cone. Although the minimum value of the spin rate for stable motion of the system in the cylindrical case has not heretofore been determined, a spin rate below 1.375 times the orbital rate has been observed to exhibit unstable behavior for long simulation times. In the conical case, all spin rates produce unstable motion. Williams and Moore[23] examined the rotating tethered satellite system in LEO and studied the dynamics of two tethered configurations: a planar ring of satellites connected through conductive tethers and a three-dimensional configuration in which the satellites are arranged in a ring whose plane is perpendicular to the nadir direction with two anchor bodies that provide a gravity-gradient restoring moment. The stability of the same three dimensional configuration that was considered by Williams and Moore[23] has been investigated by Tragesser and Tuncay[24] for the off-nadir (but still Earth-facing) orientation of the Likins–Pringle conical equilibria. Mori and Matunga[25] proposed the coordinated control of tethered satellite clusters using tether tension and thrust.

The innovative methods for control of the rotating system during stationkeeping, deployment, retrieval, reconfiguration, and techniques for tethered damping management are still required. The present study attempts to carry out such studies focused on stationkeeping, deployment, and retrieval aspects of formation flying of satellites. We consider the general formulation of a rotating system composed of three satellites connected by flexible tethers and moving in an elliptic orbit. The different masses of the satellites and different tether lengths connecting them have also been included in the formulation. We obtain the minimum value of the spin rate for the cylindrical case that was considered by Tragesser.[22] The effects of tether deployment and retrieval on the system dynamics are investigated. The Lagrangian formulation procedure is utilized to obtain the governing ordinary differential equations of motion for the proposed constrained system. Because of the relatively short tether length considered in this study, it is assumed that the tether dynamics do not affect the orbital dynamics. Next, an equilibrium analysis is undertaken to determine the necessary design limits on system parameters followed by the development of tether deployment and retrieval laws. Finally, for a detailed assessment of the proposed control strategy the set of governing equations of motion is numerically integrated.

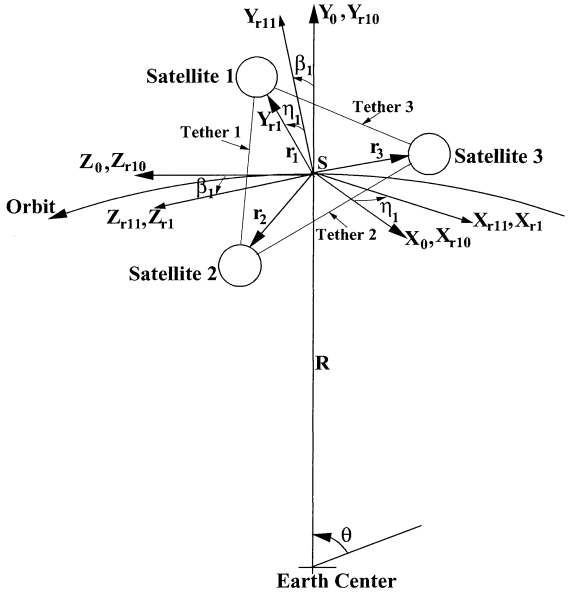

Fig. 1 Geometry of rotating tethered satellite formation.

Proposed System Model and Equations of Motion

The investigation is initiated by formulating the equations of motion of the proposed system moving in an elliptic orbit. The system model is composed of three satellites connected by tethers (Fig. 1). Satellite 1, satellite 2, and satellite 3 are treated as particles of masses m_1, m_2, and m_3, respectively. The tethers, made of a light material like Kevlar, are assumed to have negligible mass. Their damping effects and transverse vibrations are ignored. The system is assumed to be vertically above the ground station while passing over the ascending node. The corresponding nodal line represents the reference line in orbit for the measurement of the true anomaly. The coordinate frame $x_0y_0z_0$ passing through the system center of mass S represents the orbital reference frame. Here, the x_0 axis is taken along normal to the orbital plane, y_0 axis points along the local vertical, and z_0 axis represents the third axis of this right-handed frame taken. For the variable position $\boldsymbol{r}_i$ joining the system mass center S and satellite i, the angle β_i denotes rotation about the axis normal to the orbital plane and is referred as the in-plane swing or pitch angle. The resulting coordinate frame associated with this vector is denoted by $S - x_{\mathrm{ri}}y_{\mathrm{ri}}z_{\mathrm{ri}}$. This frame is obtained from the $S - x_0y_0z_0$ frame by first β_i rotation about the x_0 axis, which transforms the $S - x_0y_0z_0$ axes to the $S - x_{\mathrm{ri1}}y_{\mathrm{ri1}}z_{\mathrm{ri1}}$ axes, and this is followed by η_i rotation about z_{ri1} axis. The system under consideration has nine generalized coordinates: $\boldsymbol{r}_i$ (length r_i, angles β_i and η_i, $i = 1, 2$) and tether strains (ε_j, $j = 1, 2, 3$). These generalized variables are not independent because they are related through constraints as follows:

$$f_1 = l_1 - \left\{r_1^2 + r_2^2 - 2r_1r_2[\sin\eta_1 \sin\eta_2 + \cos\eta_1 \cos\eta_2 \cos(\beta_1 - \beta_2)]\right\}^{\frac{1}{2}} = 0 \tag{1}$$

$$f_2 = l_2 - (1/\mu_3)\left\{\mu_1^2 r_1^2 + (\mu_2 + \mu_3)^2 r_2^2 + 2\mu_1(\mu_2 + \mu_3)r_1r_2 \times [\sin\eta_1 \sin\eta_2 + \cos\eta_1 \cos\eta_2 \cos(\beta_1 - \beta_2)]\right\}^{\frac{1}{2}} = 0 \tag{2}$$

$$f_3 = l_3 - (1/\mu_3)\left\{(\mu_1 + \mu_3)^2 r_1^2 + \mu_2^2 r_2^2 + 2\mu_2(\mu_1 + \mu_3)r_1r_2 \times [\sin\eta_1 \sin\eta_2 + \cos\eta_1 \cos\eta_2 \cos(\beta_1 - \beta_2)]\right\}^{\frac{1}{2}} = 0 \tag{3}$$

where $l_j = l_{j0}(1 + \varepsilon_j)$, $j = 1, 2, 3$.

The position and orientation of satellite 3 can be obtained from the given positions and orientations of satellite 1 and satellite 2 considering the system center of mass lies at the origin of the reference

frame $S - x_{\mathrm{ri}} y_{\mathrm{ri}} z_{\mathrm{ri}}$ as

$$r_3 = \frac{1}{\mu_3}\Big\{\mu_1^2 r_1^2 + \mu_2^2 r_2^2 + 2\mu_1\mu_2 r_1 r_2[\sin\eta_1 \sin\eta_2 + \cos\eta_1 \cos\eta_2 \cos(\beta_1 - \beta_2)]\Big\}^{\frac{1}{2}} \tag{4}$$

$$\beta_3 = \cos^{-1}\left[-\frac{\mu_1 r_1 \cos\beta_1 \cos\eta_1 + \mu_2 r_2 \cos\beta_2 \cos\eta_2}{\mu_3 r_3 \cos\eta_3}\right] \tag{5}$$

$$\eta_3 = \sin^{-1}\left[\frac{\mu_1 r_1 \sin\eta_1 + \mu_2 r_2 \sin\eta_2}{\mu_3 r_3}\right] \tag{6}$$

To apply the Lagrangian approach for the formulation of the system equations of motion, the expressions for the system kinetic energy T as well as the potential energy V are first obtained:

$$\begin{aligned} T = {} & \frac{1}{2}m(\dot{R}^2 + \dot{\theta}^2 R^2) + \frac{1}{2}\sum_{i=1}^{2}\frac{m_i(m_i + m_3)}{m_3} \\ & \times \left[\dot{r}_i^2 + r_i^2(\dot{\theta} + \dot{\beta}_i)^2 \cos^2\eta_i + r_i^2\dot{\eta}_i^2\right] \\ & + \frac{m_1 m_2}{m_3}\big(r_1 r_2\{\dot{\eta}_1\dot{\eta}_2[\cos(\beta_1 - \beta_2)\sin\eta_1 \sin\eta_2 + \cos\eta_1 \cos\eta_2] \\ & + [-\dot{\eta}_1(\dot{\theta} + \dot{\beta}_2)\sin\eta_1 \cos\eta_2 + \dot{\eta}_2(\dot{\theta} + \dot{\beta}_1)\sin\eta_2 \cos\eta_1] \\ & \times \sin(\beta_1 - \beta_2) + (\dot{\theta} + \dot{\beta}_1)(\dot{\theta} + \dot{\beta}_2)\cos(\beta_1 - \beta_2)\cos\eta_1 \cos\eta_2\} \\ & + \dot{r}_1 r_2\{\dot{\eta}_2[-\cos(\beta_1 - \beta_2)\cos\eta_1 \sin\eta_2 + \sin\eta_1 \cos\eta_2] \\ & + (\dot{\theta} + \dot{\beta}_2)\sin(\beta_1 - \beta_2)\cos\eta_1 \cos\eta_2\} \\ & + r_1\dot{r}_2\{\dot{\eta}_1[-\cos(\beta_1 - \beta_2)\cos\eta_2 \sin\eta_1 + \sin\eta_2 \cos\eta_1] \\ & + (\dot{\theta} + \dot{\beta}_1)\sin(\beta_2 - \beta_1)\cos\eta_1 \cos\eta_2\} \\ & + \dot{r}_1\dot{r}_2[\cos(\beta_1 - \beta_2)\cos\eta_1 \cos\eta_2 + \sin\eta_1 \sin\eta_2]\big) \end{aligned} \tag{7}$$

$$\begin{aligned} V = {} & -\frac{GM_e m}{R} + \frac{1}{2}\frac{GM_e}{R^3}\sum_{i=1}^{2}\left[\frac{m_i(m_i + m_3)}{m_3}r_i^2\left(1 - 3\cos^2\beta_i \cos^2\eta_i\right)\right] \\ & + \frac{GM_e}{R^3}\frac{m_1 m_2}{m_3}r_1 r_2[\cos(\beta_1 - \beta_2)\cos\eta_1 \cos\eta_2 + \sin\eta_1 \sin\eta_2 \\ & - 3\cos\beta_1 \cos\eta_1 \cos\beta_2 \cos\eta_2] + \frac{1}{2}EA\sum_{j=1}^{3} l_{\mathrm{jo}}\varepsilon_j^2 u_j \end{aligned} \tag{8}$$

The term u_j in the potential energy expression is simply a unit function, the use of which precludes any negative strain in the tether. The potential energy V is an approximate expression considering the term till $\mathcal{O}(1/R^4)$.

The Lagrangian equations of motion corresponding to the various generalized coordinates indicated earlier can be obtained using the general relation

$$\frac{\mathrm{d}}{\mathrm{d}t}\left(\frac{\partial T}{\partial \dot{q}}\right) - \frac{\partial T}{\partial q} + \frac{\partial V}{\partial q} = \sum_{i=1}^{3}\Lambda_i\frac{\partial f_i}{\partial q} \tag{9}$$

where q = the generalized coordinate, $(r_i, \beta_i, \eta_i, i = 1, 2, \varepsilon_j, j = 1, 2, 3)$ and Λ_i = Lagrange multiplier corresponding to ith constraint as indicated in Eqs. (1–3). We substitute the generalized coordinates in the preceding equations and express the derivative with respect to true anomaly using the relations given here:

$$\dot{q} = \dot{\theta}q' = \left[\sqrt{\mu a(1 - e^2)}\Big/R^2\right]q'$$

$$\ddot{q} = (\mu/R^3)[(1 + e\cos\theta)q'' - 2e\sin\theta]$$

By replacing the orbital radius R in terms of semimajor axis and eccentricity using the relation

$$R = \frac{a(1 - e^2)}{(1 + e\cos\theta)} = \frac{\mu^{\frac{1}{3}}(1 - e^2)}{\Omega^{\frac{2}{3}}(1 + e\cos\theta)}$$

and carrying out the algebraic manipulations, we get the following governing nonlinear, coupled ordinary differential equations of motion:

1) r_i equation, $i = 1, 2$

$$\begin{aligned} & (1 + e\cos\theta)r_i'' + m_{\mathrm{ri}}(1 + e\cos\theta)[\cos(\beta_i - \beta_k)\cos\eta_i \cos\eta_k \\ & + \sin\eta_i \sin\eta_k]r_k'' + m_{\mathrm{ri}}r_k(1 + e\cos\theta)\sin(\beta_i - \beta_k) \\ & \times \cos\eta_i \cos\eta_k\beta_k'' + m_{\mathrm{ri}}r_k(1 + e\cos\theta)[\sin\eta_i \cos\eta_k \\ & - \cos\eta_i \sin\eta_k \cos(\beta_i - \beta_k)]\eta_k'' - 2e\sin\theta \\ & \times \big(r_i' + m_{\mathrm{ri}}[\cos(\beta_i - \beta_k)\cos\eta_i \cos\eta_k + \sin\eta_i \sin\eta_k]r_k' \\ & + m_{\mathrm{ri}}r_k\{(1 + \beta_k')\sin(\beta_i - \beta_k)\cos\eta_i \cos\eta_k \\ & + \eta_k'[\sin\eta_i \cos\eta_k - \cos\eta_i \sin\eta_k \cos(\beta_i - \beta_k)]\}\big) \\ & + m_{\mathrm{ri}}(1 + e\cos\theta)\big(2r_k'\{(1 + \beta_k')\sin(\beta_i - \beta_k)\cos\eta_i \cos\eta_k \\ & + \eta_k'[\sin\eta_i \cos\eta_k - \cos(\beta_i - \beta_k)\cos\eta_i \sin\eta_k]\} \\ & + r_k\{-2\eta_k'(1 + \beta_k')\sin(\beta_i - \beta_k)\cos\eta_i \sin\eta_k \\ & - \eta_k'^2[\sin\eta_i \sin\eta_k + \cos(\beta_i - \beta_k)\cos\eta_i \cos\eta_k] \\ & - (1 + \beta_k')^2\cos(\beta_i - \beta_k)\cos\eta_i \cos\eta_k\}\big) - (1 + e\cos\theta)r_i \\ & \times \left[(1 + \beta_i')^2\cos^2\eta_i + \eta_i'^2\right] + r_i\left(1 - 3\cos^2\beta_i \cos^2\eta_i\right) \\ & + m_{\mathrm{ri}}r_k[\cos(\beta_i - \beta_k)\cos\eta_i \cos\eta_k + \sin\eta_i \sin\eta_k \\ & - 3\cos\beta_i \cos\eta_i \cos\beta_k \cos\eta_k] + (\lambda_1/l_1)\{\mu_3/[\mu_i(\mu_i + \mu_3)]\} \\ & \times \{r_i - r_k[\cos(\beta_i - \beta_k)\cos\eta_i \cos\eta_k + \sin\eta_i \sin\eta_k]\} \\ & + [\lambda_2/(l_2\mu_3)]\{p_{\mathrm{ii}}r_i + q_{\mathrm{ik}}r_k[\cos(\beta_i - \beta_k)\cos\eta_i \cos\eta_k \\ & + \sin\eta_i \sin\eta_k]\} + [\lambda_3/(l_3\mu_3)]\{p_{\mathrm{ik}}r_i + q_{\mathrm{ii}}r_k[\cos(\beta_i - \beta_k) \\ & \times \cos\eta_i \cos\eta_k + \sin\eta_i \sin\eta_k]\} = 0 \end{aligned} \tag{10}$$

2) β_i equation, $i = 1, 2$

$$\begin{aligned} & -m_{\mathrm{ri}}(1 + e\cos\theta)r_i \sin(\beta_i - \beta_k)\cos\eta_i \cos\eta_k r_k'' + r_i^2(1 + e\cos\theta) \\ & \times \cos^2\eta_i\beta_i'' + m_{\mathrm{ri}}r_i r_k(1 + e\cos\theta)\cos(\beta_i - \beta_k)\cos\eta_i \cos\eta_k\beta_k'' \\ & + m_{\mathrm{ri}}r_i r_k(1 + e\cos\theta)\cos\eta_i \sin\eta_k \sin(\beta_i - \beta_k)\eta_k'' \\ & - 2e\sin\theta\big[-m_{\mathrm{ri}}r_i \sin(\beta_i - \beta_k)\cos\eta_i \cos\eta_k r_k' \\ & + r_i^2\cos^2\eta_i(1 + \beta_i') + m_{\mathrm{ri}}r_i r_k\cos(\beta_i - \beta_k)\cos\eta_i \cos\eta_k \\ & \times (1 + \beta_k') + m_{\mathrm{ri}}r_i r_k\cos\eta_i \sin\eta_k \sin(\beta_i - \beta_k)\eta_k'\big] \\ & + (1 + e\cos\theta)(1 + \beta_i')\big[2r_i r_i'\cos^2\eta_i - r_i^2\sin(2\eta_i)\eta_i'\big] \\ & + m_{\mathrm{ri}}(1 + e\cos\theta)r_i\cos\eta_i\big\{2r_k'[(1 + \beta_k')\cos(\beta_i - \beta_k)\cos\eta_k \\ & + \eta_k'\sin(\beta_i - \beta_k)\sin\eta_k] + r_k\big[-2\eta_k'(1 + \beta_k')\cos(\beta_i - \beta_k)\sin\eta_k \\ & + \eta_k'^2\sin(\beta_i - \beta_k)\cos\eta_k + (1 + \beta_k')^2\sin(\beta_i - \beta_k)\cos\eta_k\big]\big\} \\ & + 3r_i^2\cos\beta_i \sin\beta_i \cos^2\eta_i + m_{\mathrm{ri}}r_i r_k\cos\eta_i \\ & \times [-\sin(\beta_i - \beta_k)\cos\eta_k + 3\sin\beta_i \cos\beta_k \cos\eta_k] \\ & + \{(\lambda_1/l_1)\{\mu_3/[\mu_i(\mu_i + \mu_3)]\} - [\lambda_2/(l_2\mu_3)]q_{\mathrm{ik}} \\ & - [\lambda_3/(l_3\mu_3)]q_{\mathrm{ii}}\}r_i r_k\cos\eta_i \cos\eta_k \sin(\beta_i - \beta_k) = 0 \end{aligned} \tag{11}$$

3) η_i equation, $i = 1, 2$

$$
\begin{aligned}
&m_{ri}(1 + e\cos\theta)r_i[-\cos(\beta_i - \beta_k)\sin\eta_i\cos\eta_k + \cos\eta_i\sin\eta_k]r_k'' \\
&\quad - m_{ri}r_ir_k(1 + e\cos\theta)\sin(\beta_i - \beta_k)\sin\eta_i\cos\eta_k\beta_k'' \\
&\quad + r_i^2(1 + e\cos\theta)\eta_i'' + m_{ri}r_ir_k(1 + e\cos\theta)[\cos\eta_i\cos\eta_k \\
&\quad + \sin\eta_i\sin\eta_k\cos(\beta_i - \beta_k)]\eta_k'' - 2e\sin\theta\big\{m_{ri}r_i[-\cos(\beta_i - \beta_k) \\
&\quad \times \sin\eta_i\cos\eta_k + \cos\eta_i\sin\eta_k]r_k' - m_{ri}r_ir_k\sin(\beta_i - \beta_k) \\
&\quad \times \sin\eta_i\cos\eta_k(1 + \beta_k') + r_i^2\eta_i' + m_{ri}r_ir_k[\cos\eta_i\cos\eta_k \\
&\quad + \sin\eta_i\sin\eta_k\cos(\beta_i - \beta_k)]\eta_k'\big\} + 2(1 + e\cos\theta)r_ir_i'\eta_i' \\
&\quad + m_{ri}(1 + e\cos\theta)r_i\big(2r_k'\{-(1 + \beta_k')\sin(\beta_i - \beta_k)\sin\eta_i\cos\eta_k \\
&\quad + \eta_k'[\cos(\beta_i - \beta_k)\sin\eta_i\sin\eta_k + \cos\eta_i\cos\eta_k]\} \\
&\quad + r_k\big\{2\eta_k'(1 + \beta_k')\sin(\beta_i - \beta_k)\sin\eta_i\sin\eta_k \\
&\quad + \eta_k'^2[\cos(\beta_i - \beta_k)\sin\eta_i\cos\eta_k - \cos\eta_i\sin\eta_k]\big\} \\
&\quad + (1 + \beta_k')^2\cos(\beta_i - \beta_k)\sin\eta_i\cos\eta_k\big) + (1 + e\cos\theta)r_i^2 \\
&\quad \times (1 + \beta_i')^2\sin\eta_i\cos\eta_i + 3r_i^2\cos^2\beta_i\cos\eta_i\sin\eta_i \\
&\quad + m_{ri}r_ir_k[-\cos(\beta_i - \beta_k)\sin\eta_i\cos\eta_k + \cos\eta_i\sin\eta_k \\
&\quad + 3\cos\beta_i\sin\eta_i\cos\beta_k\cos\eta_k] - \{(\lambda_1/l_1)\{\mu_3/[\mu_i(\mu_i + \mu_3)]\} \\
&\quad - [\lambda_2/(l_2\mu_3)]q_{ik} - [\lambda_3/(l_3\mu_3)]q_{ii}\}r_ir_k[-\cos(\beta_i - \beta_k) \\
&\quad \times \sin\eta_i\cos\eta_k + \cos\eta_i\sin\eta_k] = 0
\end{aligned}
\tag{12}
$$

4) Tether strain (ε_i), $i = 1, 2, 3$

$$C_il_{i0} - \lambda_il_{i0} = 0 \tag{13}$$

where the subscript $k = 2$ if $i = 1$; $k = 1$ if $i = 2$;

$$m_{r1} = \frac{\mu_2}{\mu_1 + \mu_3}, \qquad m_{r2} = \frac{\mu_1}{\mu_2 + \mu_3}, \qquad p_{11} = \frac{\mu_1}{\mu_1 + \mu_3}$$

$$p_{12} = \frac{1}{p_{11}}, \qquad p_{21} = \frac{\mu_2}{\mu_2 + \mu_3}, \qquad p_{22} = \frac{1}{p_{21}}, \qquad q_{11} = \frac{\mu_2}{\mu_1}$$

$$q_{12} = \frac{\mu_2 + \mu_3}{\mu_1 + \mu_3}, \qquad q_{21} = \frac{1}{q_{11}}, \qquad q_{22} = \frac{1}{q_{12}}, \qquad C = \frac{EA}{m\Omega^2}$$

$$\lambda_i = \left[\frac{1}{m\Omega^2}\right]\left[\frac{1 - e^2}{1 + e\cos\theta}\right]^3\Lambda_i, \qquad i = 1, 2, 3$$

$$C_i = C\left[\frac{1 - e^2}{1 + e\cos\theta}\right]^3\varepsilon_iu_i, \qquad i = 1, 2, 3$$

The expressions for λ_1, λ_2, and λ_3 obtained from Eq. (13) are substituted in Eqs. (10–12). The resulting equations are the equations of motion of the proposed tether system with r_i, β_i, and η_i, $i = 1, 2$ as independent coordinates or degrees of freedom of the system.

Equilibrium Analysis

We first consider the simple case of the system comprised of equal satellite masses and tether lengths, that is, $\mu_1 = \mu_2 = \mu_3 = \frac{1}{3}$ and $l_{10} = l_{20} = l_{30} = l_{t0}$, moving in a circular orbit. We derive the conditions of feasible steady-spin motion for such systems, and then we generalize the procedure to the case when satellite masses and tether lengths are different. Here, by steady-spin motion we mean that the system spins with a constant average spin rate. For the system positioned in an arbitrary instantaneous equilibrium configuration and rotating in an orbital plane given by, say,

$$e = 0, \qquad r_i = r_{ie}, \qquad \beta_i = \beta_{ie}, \qquad \beta_i' = \beta_{ie}' = \beta_e'$$
$$\eta_i = 0, \qquad \eta_i' = \eta_{ie}' = 0$$

a substitution of the instantaneous equilibrium conditions

$$r_i = r_{ie}, \qquad r_i' = r_i'' = 0, \qquad \beta_i = \beta_{ie}, \qquad \beta_i' = \beta_{ie}' = \beta_e'$$
$$\beta_i'' = 0, \qquad \eta_i = 0, \qquad \eta_i' = \eta_{ie}' = 0, \qquad \eta_i'' = 0, \qquad (i = 1, 2)$$

into Eqs. (1–3) and Eqs. (10–13) leads to the seven algebraic nonlinear transcendental equations. For the case when satellite 1 is at the vertex facing outward along the local vertical, that is, $\beta_{1e} = 0$, we get a closed-form solution as follows:

$$\frac{\lambda_{je}}{l_{je}} = \frac{1}{9}\big[(1 + \beta_e')^2 + 2\big], \qquad j = 1, 3 \tag{14}$$

$$\frac{\lambda_{2e}}{l_{2e}} = \frac{1}{9}\left[(1 + \beta_e')^2 - \frac{5}{2}\right] \tag{15}$$

$$\varepsilon_{je} = \frac{(\lambda_{je}/l_{je})l_{t0}}{C - (\lambda_{je}/l_{je})l_{t0}}, \qquad j = 1, 2, 3 \tag{16}$$

$$l_{je} = \frac{l_{t0}}{1 - \lambda_{je}/(l_{je}C)}, \qquad j = 1, 2, 3 \tag{17}$$

$$r_{1e} = \frac{1}{3}\big[-l_{2e}^2 + 2\big(l_{1e}^2 + l_{3e}^2\big)\big]^{\frac{1}{2}} \tag{18}$$

$$r_{2e} = \frac{1}{3}\big[-l_{3e}^2 + 2\big(l_{1e}^2 + l_{2e}^2\big)\big]^{\frac{1}{2}} \tag{19}$$

$$\beta_{2e} = \cos^{-1}\left[-\frac{r_{1e}}{2r_{2e}}\right] \tag{20}$$

While the system is in the steady-state rotation, its configuration changes, and thereby tensions in the tethers undergo changes. As we see from the relations (14) and (15), when $\beta_{1e} = 0$ deg (i.e., satellite 1 is at the vertex), tether 1 and tether 3 have always positive tension values for any arbitrary system spin rate while tether 2, which is along the local horizontal connecting the satellite 2 and satellite 3, can get slacked if the spin rate is not sufficient. We get the following relations for tether tensions in other steady-state positions:

1) $\beta_{1e} = 30$ deg

$$\lambda_{1e}/l_{1e} = \tfrac{1}{9}\big[(1 + \beta_e')^2 + \tfrac{7}{2}\big] \tag{21}$$

$$\lambda_{je}/l_{je} = \tfrac{1}{9}\big[(1 + \beta_e')^2 - 1\big], \qquad j = 2, 3 \tag{22}$$

2) $\beta_{1e} = 60$ deg

$$\lambda_{je}/l_{je} = \tfrac{1}{9}\big[(1 + \beta_e')^2 + 2\big], \qquad j = 1, 2 \tag{23}$$

$$\lambda_{3e}/l_{3e} = \tfrac{1}{9}\big[(1 + \beta_e')^2 - \tfrac{5}{2}\big] \tag{24}$$

3) $\beta_{1e} = 90$ deg

$$\lambda_{je}/l_{je} = \tfrac{1}{9}\big[(1 + \beta_e')^2 - 1\big], \qquad j = 1, 3 \tag{25}$$

$$\lambda_{2e}/l_{2e} = \tfrac{1}{9}\big[(1 + \beta_e')^2 + \tfrac{7}{2}\big] \tag{26}$$

4) $\beta_{1e} = 120$ deg

$$\lambda_{1e}/l_{1e} = \tfrac{1}{9}\big[(1 + \beta_e')^2 - \tfrac{5}{2}\big] \tag{27}$$

$$\lambda_{je}/l_{je} = \tfrac{1}{9}\big[(1 + \beta_e')^2 + 2\big], \qquad j = 2, 3 \tag{28}$$

5) $\beta_{1e} = 150$ deg

$$\lambda_{je}/l_{je} = \tfrac{1}{9}\left[(1+\beta'_e)^2 - 1\right], \qquad j = 1, 2 \tag{29}$$

$$\lambda_{3e}/l_{3e} = \tfrac{1}{9}\left[(1+\beta'_e)^2 + \tfrac{7}{2}\right] \tag{30}$$

It can be stated from Eqs. (14) and (15) and Eqs. (21–30) that the tension in tether 1 first increases and attains the maximum value at $\beta_{1e} = 30$ deg and then it decreases and reaches to the minimum value at $\beta_{1e} = 120$ deg while the tension in tether 2 is the lowest at $\beta_{1e} = 0$ deg, and it then increases and gets the maximum value at $\beta_{1e} = 90$ deg. For tether 3, its tension first decreases and attains the lowest value at $\beta_{1e} = 60$ deg, and then it increases and gets the maximum value at $\beta_{1e} = 150$ deg. After 180 deg of phase difference, the tether tensions repeat.

To have stable steady-spin motion of the system, all three tethers must remain taut throughout the system rotational motion. Therefore, the condition of system steady-spin motion can be stated as

$$\lambda_{je}/l_{je} > 0 \qquad j = 1, 2, 3 \tag{31}$$

$$C > (\lambda_{je}/l_{je})l_{t0} \qquad j = 1, 2, 3 \tag{32}$$

Relations (31) and (32) lead to the following conditions for steady-spin motion:

$$\beta'_e > \sqrt{\tfrac{5}{2}} - 1 \qquad \text{or} \qquad \beta'_e < -\sqrt{\tfrac{5}{2}} - 1 \tag{33}$$

$$C > \tfrac{1}{9}\left[(1+\beta'_e)^2 + \tfrac{7}{2}\right] l_{t0} \tag{34}$$

Thus, we can expect steady-spin motion if the system is rotating with the spin rate just a little bit greater than the half of the orbital rate (i.e.,$\beta'_e > 0.581$), and in the case when the system is rotating opposite to the orbital motion it should spin greater than 2.581 times the orbital rate. Here, β'_e is measured with respect to the orbital frame, and therefore the spin rate required for system steady-spin motion when rotating opposite to the orbital motion is different by two. It is interesting to observe that the spin rate larger than the orbital rate as considered by DeCou[15–17] and Tragesser[22] is not required for stable system motion.

Now, we extend the preceding procedure to include the case with different satellite masses and tether lengths as well. For the system when satellite 1 is at the vertex facing outward along the local vertical, that is, $\beta_{1e} = 0$, we get the solution as follows:

$$\frac{\lambda_{je}}{l_{je}} = \mu_1\mu_k\left[(1+\beta'_e)^2 + 2\right], \qquad j = 1, 3, \qquad \text{if}$$

$$j = 1, \qquad k = 2, \qquad \text{if} \qquad j = 3, \qquad k = 3 \tag{35}$$

$$\frac{\lambda_{2e}}{l_{2e}} = \mu_2\mu_3\left[(1+\beta'_e)^2 - 1 - \frac{3\mu_1}{\mu_2+\mu_3}\right] \tag{36}$$

$$\varepsilon_{je} = \frac{(\lambda_{je}/l_{je})l_{j0e}}{C - (\lambda_{je}/l_{je})l_{j0e}}, \qquad j = 1, 2, 3 \tag{37}$$

$$l_{je} = \frac{l_{j0e}}{1 - \lambda_{je}/(l_{je}C)}, \qquad j = 1, 2, 3 \tag{38}$$

$$r_{1e} = \left[-\mu_2\mu_3 l_{2e}^2 + (\mu_2+\mu_3)\left(\mu_2 l_{1e}^2 + \mu_3 l_{3e}^2\right)\right]^{\frac{1}{2}} \tag{39}$$

$$r_{2e} = \left[-\mu_3\mu_1 l_{3e}^2 + (\mu_3+\mu_1)\left(\mu_3 l_{2e}^2 + \mu_1 l_{1e}^2\right)\right]^{\frac{1}{2}} \tag{40}$$

$$\beta_{2e} = \cos^{-1}\left[-\frac{r_{1e}\mu_1}{r_{2e}(\mu_2+\mu_3)}\right] \tag{41}$$

with the condition on tether lengths

$$l_{1e}^2 + \frac{(\mu_2-\mu_3)}{(\mu_2+\mu_3)} l_{2e}^2 = l_{3e}^2 \tag{42}$$

In terms of unstretched tether lengths, the preceding relation (42) can be written as

$$\frac{l_{10,e}^2}{[1-\lambda_{1e}/(l_{1e}C)]^2} + \frac{(\mu_2-\mu_3)l_{20,e}^2}{(\mu_2+\mu_3)[1-\lambda_{2e}/(l_{2e}C)]^2} = \frac{l_{30,e}^2}{[1-\lambda_3/(l_{3e}C)]^2} \tag{43}$$

As per Eq. (43), if all of the three satellites have equal masses (i.e., $\mu_1 = \mu_2 = \mu_3 = \frac{1}{3}$) or even satellite 2 and satellite 3 have the same masses (i.e., $\mu_2 = \mu_3$), the tether length $l_{10,e}$ has to be equal to tether length $l_{30,e}$ with an arbitrary choice on the tether length $l_{20,e}$. For the case when $\mu_1 \neq \mu_2 \neq \mu_3$ or even $\mu_2 \neq \mu_3$, if any two tether lengths, say, $l_{10,e}$ and $l_{20,e}$, are given then third tether length, $l_{30,e}$ has to be determined from Eq. (43). We get the following relations for tether tensions in other steady-state positions:

1) $\beta_{1e} = 30$ deg

$$\lambda_{1e}/l_{1e} = \mu_1\mu_2\left[(1+\beta'_e)^2 + 2 + 3\mu_3/(\mu_1+\mu_2)\right] \tag{44}$$

$$\lambda_{je}/l_{je} = \mu_k\mu_3\left[(1+\beta'_e)^2 - 1\right], \qquad j = 2, 3, \qquad \text{if}$$

$$j = 2, \qquad k = 2, \qquad \text{if} \qquad j = 3, \qquad k = 1 \tag{45}$$

2) $\beta_{1e} = 60$ deg

$$\lambda_{je}/l_{je} = \mu_k\mu_2\left[(1+\beta'_e)^2 + 2\right], \qquad j = 1, 2, \qquad \text{if}$$

$$j = 1, \qquad k = 1, \qquad \text{if} \qquad j = 2, \qquad k = 3 \tag{46}$$

$$\lambda_{3e}/l_{3e} = \mu_1\mu_3\left[(1+\beta'_e)^2 - 1 - 3\mu_2/(\mu_1+\mu_3)\right] \tag{47}$$

3) $\beta_{1e} = 90$ deg

$$\lambda_{je}/l_{je} = \mu_k\mu_1\left[(1+\beta'_e)^2 - 1\right], \qquad j = 1, 3, \qquad \text{if}$$

$$j = 1, \qquad k = 2, \qquad \text{if} \qquad j = 3, \qquad k = 3 \tag{48}$$

$$\lambda_{2e}/l_{2e} = \mu_2\mu_3\left[(1+\beta'_e)^2 + 2 + 3\mu_1/(\mu_2+\mu_3)\right] \tag{49}$$

4) $\beta_{1e} = 120$ deg

$$\lambda_{1e}/l_{1e} = \mu_1\mu_2\left[(1+\beta'_e)^2 - 1 - 3\mu_3/(\mu_1+\mu_2)\right] \tag{50}$$

$$\lambda_{je}/l_{je} = \mu_k\mu_3\left[(1+\beta'_e)^2 + 2\right], \qquad j = 2, 3, \qquad \text{if}$$

$$j = 2, \qquad k = 2, \qquad \text{if} \qquad j = 3, \qquad k = 1 \tag{51}$$

5) $\beta_{1e} = 150$ deg

$$\lambda_{je}/l_{je} = \mu_k\mu_2\left[(1+\beta'_e)^2 - 1\right], \qquad j = 1, 2, \qquad \text{if}$$

$$j = 1, \qquad k = 1 \qquad \text{if} \qquad j = 2, \qquad k = 3 \tag{52}$$

$$\lambda_{3e}/l_{3e} = \mu_1\mu_3\left[(1+\beta'_e)^2 + 2 + 3\mu_2/(\mu_1+\mu_3)\right] \tag{53}$$

Therefore, we can write the condition of system steady-spin motion as

$$\beta'_e > \sqrt{1 + 3\mu_i/(1-\mu_i)} - 1, \qquad i = 1, 2, 3 \tag{54}$$

$$C > \mu_j\mu_k\left[(1+\beta'_e)^2 + 2 + 3\mu_j/(1-\mu_j)\right] l_{j0,e}, \qquad j = 1, 2, 3$$

$$\text{if} \qquad j = 1, \qquad k = 2, \qquad \text{if} \qquad j = 2, \qquad k = 3$$

$$\text{if} \qquad j = 3, \qquad k = 1 \tag{55}$$

In the case whereas the system is rotating opposite to the orbital motion, we get the conditions for steady-spin motion as follows:

$$\beta'_e < -\sqrt{1 + 3\mu_i/(1-\mu_i)} - 1, \qquad i = 1, 2, 3 \tag{56}$$

and Eq. (55).

Conditions (54) and (56) are dependent on satellite mass ratios (in particular, the mass of the heaviest satellite), whereas these conditions are independent of the orbital radius and tether length. The condition (55) states the relation between C, which is a function of tether rigidity, mean orbital angular velocity, and total system mass, and mass ratio, tether length, and the system spin rate. It can be stated from these conditions (54–56) that the system spin rate requirement stated by condition (33) is the minimum spin rate [i.e.,$(\beta_0')_{\rm cr} = 0.581$ or -2.581] for any combinations of satellite mass ratios.

Deployment and Retrieval of Tethers

Various tether deployment and retrieval laws[10–12] have been developed in the literature. These schemes use a tether rate that is mainly exponentially increasing/decreasing or uniform or a combination of these (i.e., exponential uniform, exponential uniform exponential, exponential exponential). However, in the case of tether retrieval it is not possible to have the final commanded tether length retrieval rate zero using the single-stage and multistage schemes[10–12] and while applying multistage schemes[10–12] the tether length retrieval rate cannot be the same at transition. These problems can cause sudden excitation of system response at the end of retrieval using the single-stage schemes and at transition with multistage schemes. To avoid these problems, we consider the following tether deployment/ retrieval law:

$$l_{j0} = l_{j0,i} + (l_{j0,f} - l_{j0,i}) \sin[(\theta - \theta_{r0})/(4\tau)] \qquad \text{if}$$
$$0 \le (\theta - \theta_{r0}) < 2\pi\tau, \qquad j = 1, 2, 3$$
$$l_{j0} = l_{j0,f} \qquad \text{if} \qquad 2\pi\tau \le (\theta - \theta_{r0}), \qquad j = 1, 2, 3 \tag{57}$$

The commanded tether length rate is

$$l'_{j0} = (1/4\tau)(l_{j0,f} - l_{j0,i}) \cos[(\theta - \theta_{r0})/(4\tau)] \qquad \text{if}$$
$$0 \le (\theta - \theta_{r0}) < 2\pi\tau, \qquad j = 1, 2, 3$$
$$l'_{j0} = 0 \qquad \text{if} \qquad 2\pi\tau \le (\theta - \theta_{r0}), \qquad j = 1, 2, 3 \tag{58}$$

Here, τ represents the number of orbits allowed for completing the desired tether length changes.

In the case of tether deployment/ retrieval, the system might experience changes in its spin rate that can lead to slackening of tethers and thus system instability. To find the conditions of system steady-spin motion in such situations, we consider the system, for simplicity, moving in a circular orbit of angular velocity ω_c and all three satellites in the orbital plane having the rotational velocity of β_0' with the initial condition of satellite 1 at the vertex facing outward along the local vertical, that is, $\beta_{10} = \eta_{10} = \eta_{20} = 0$, $\beta_{20} = \beta_{2e}$, $\beta'_{10} = \beta'_{20} = \beta'_0 = \beta'_e$, and $\eta'_{1e} = \eta'_{2e} = 0$. The initial angular momentum of the system H_0 can be written as

$$H_0 = mR^2\omega_c + \left(m_1 r_1^2 + m_2 r_2^2 + m_3 r_3^2\right)\omega_c(1 + \beta_0') \tag{59}$$

The preceding relation (59) can be expressed in terms of tether lengths using Eqs. (1–4) as follows:

$$H_0 = mR^2\omega_c + m\left(\mu_1\mu_2 l_1^2 + \mu_2\mu_3 l_2^2 + \mu_3\mu_1 l_3^2\right)\omega_c(1 + \beta_0') \tag{60}$$

The relation (60) can be approximately expressed in terms of unstretched tether lengths as

$$H_0 = mR^2\omega_c + m\left(\mu_1\mu_2 l_{10,i}^2 + \mu_2\mu_3 l_{20,i}^2 + \mu_3\mu_1 l_{30,i}^2\right)\omega_c(1 + \beta_0') \tag{61}$$

Applying the tether deployment/retrieval law, the tether length $l_{j0,i}$ is changed to $l_{j0,f}$, $i = 1, 2, 3$. Let the system now rotate about its mass center with an angular velocity of β'_f. The angular momentum of the system H_f is given as

$$H_f = mR^2\omega_c + m\left(\mu_1\mu_2 l_{10,f}^2 + \mu_2\mu_3 l_{20,f}^2 + \mu_3\mu_1 l_{30,f}^2\right)\omega_c(1 + \beta_f') \tag{62}$$

Assuming conservation of angular momentum, we have $H_0 = H_f$. This fact leads to the following relation:

$$\beta_f' = \left\{\frac{\mu_1\mu_2 l_{10,i}^2 + \mu_2\mu_3 l_{20,i}^2 + \mu_3\mu_1 l_{30,i}^2}{\mu_1\mu_2 l_{10,f}^2 + \mu_2\mu_3 l_{20,f}^2 + \mu_3\mu_1 l_{30,f}^2}\right\}(1 + \beta_0') - 1 \tag{63}$$

It is to be observed from relation (63) that in the case of tether deployment the system spin rate decreases and thereby the tethers can become loosened and have decreased tension. Even with the initial situation of all of the tethers being taut, they can get slackened during the deployment phase in the case of a large increase in tether lengths when the system spin rate decreases below the critical spin rate needed for system steady-spin motion, and so it prohibits the applicability of any arbitrarily large tether deployment rate. However, it is possible to choose such an initial spin rate of the system so that even at the end of a large tether deployment the system spin rate is above the critical spin rate and tethers remain taut. The tether deployment rate has to be indeed slow for achieving stable steady-spin motion of the system during the deployment phase. Using the conditions of steady-spin motion [Eqs. (54) and (56)] obtained in the preceding section, we can obtain the conditions of system steady-spin motion for tether deployment phase as follows:

$$\beta_0' > \left\{\frac{\mu_1\mu_2 l_{10,f}^2 + \mu_2\mu_3 l_{20,f}^2 + \mu_3\mu_1 l_{30,f}^2}{\mu_1\mu_2 l_{10,i}^2 + \mu_2\mu_3 l_{20,i}^2 + \mu_3\mu_1 l_{30,i}^2}\right\}\sqrt{1 + \frac{3\mu_i}{1 - \mu_i}} - 1$$
$$i = 1, 2, 3 \tag{64}$$

and Eq. (55).

For the case where the system is rotating opposite to the orbital motion, the conditions for system steady-spin motion in the deployment phase are obtained as

$$\beta_0' < -\left\{\frac{\mu_1\mu_2 l_{10,f}^2 + \mu_2\mu_3 l_{20,f}^2 + \mu_3\mu_1 l_{30,f}^2}{\mu_1\mu_2 l_{10,i}^2 + \mu_2\mu_3 l_{20,i}^2 + \mu_3\mu_1 l_{30,i}^2}\right\}\sqrt{1 + \frac{3\mu_i}{1 - \mu_i}} - 1$$
$$i = 1, 2, 3 \tag{65}$$

and Eq. (55).

The conditions of deployment stated by Eqs. (55), (65), and (66) simply imply the constant tether length conditions to the deployed system and do not account for the dynamics of the deployment, which can be destabilizing. In the case of tether retrieval, we can find from the relation (63) that the system spin rate increases, and thereby the tethers can become more taut and have increased tension. With the initial situation of all of the tethers being taut, they remain taut throughout the retrieval phase provided the rate of retrieval is relatively slow. Therefore, the conditions of system steady-spin motion for tether retrieval are the same as obtained in Eqs. (54–56). However, the large decrease in tether lengths can result in very high tether tension because of the increase in system spin rate, and so it might prohibit the applicability of any arbitrarily large tether retrieval rate.

Results and Discussion

To study the performance of the proposed system, the detailed system response is numerically simulated using Eqs. (1–3), (10–13), and (57) with the initial conditions of $r_{10} = r_{1e}$, $r_{20} = r_{2e}$, $r'_{10} = r'_{20} = 0$, $\beta_{10} = \eta_{10} = \eta_{20} = 0$, $\beta_{20} = \beta_{2e}$, $\beta'_{10} = \beta'_{20} = \beta'_0 = \beta'_e$, $l_{10,e} = l_{20,e} = l_{r0}$. The values of the parameters r_{1e}, r_{2e}, β_{2e}, and l_{30e} are obtained using Eqs. (39–41) and (43). For known starting values of independent variables $r_{i0}, r'_{i0}, \beta_{i0}, \eta_{i0}, \beta'_{i0}$, and η'_{i0} $(i = 1, 2)$ at each step of numerical integration, we first solve for dependent variables ε_1, ε_2, and ε_3 using the constraint relations (1–3). The substitution of these dependent variables into Eq. (13) enables the determination of λ_i, $i = 1, 2, 3$. The values of the dependent variables $(\varepsilon_1, \varepsilon_2, \varepsilon_3)$ and λ_i, $i = 1, 2, 3$, thus, explicitly available are utilized to compute the new values of the variables at the end of the step through integration of the set of the differential equations (10–12). The integration

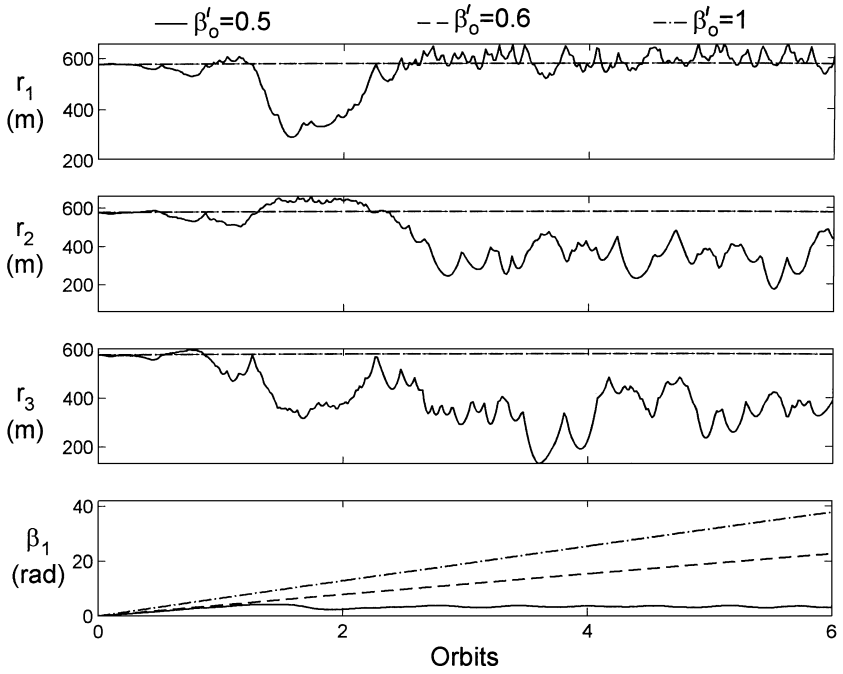

Fig. 2 Typical system response as affected by in-plane swing rates β_0': $e = 0$, $C_t = 10^5$, $l_{t0} = 1$ km, $\mu_1 = \mu_2 = \mu_3 = \frac{1}{3}$, $\eta_0' = 0$.

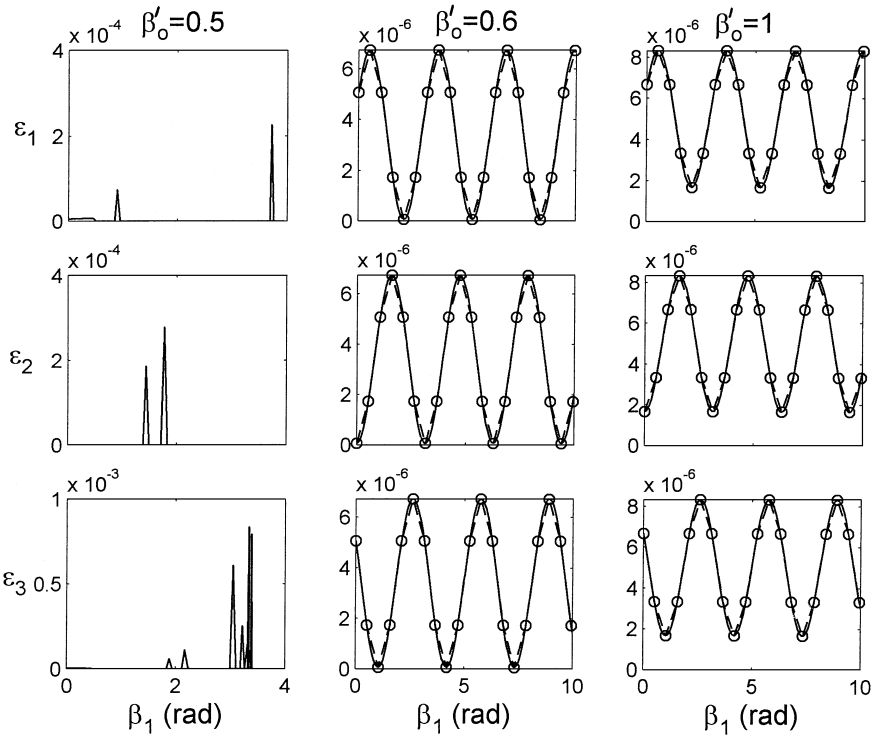

Fig. 3 Effects of in-plane swing rates β_0' on tether strains: $e = 0$, $C_t = 10^5$, $l_{t0} = 1$ km, $\mu_1 = \mu_2 = \mu_3 = \frac{1}{3}$, and $\eta_0' = 0$; ——, numerical solution and - - - -, analytical solution with calculation at discrete points marked by ○.

is carried out using the International Mathematical and Statistical Library routine DDASPG based on the Petzoid–Gear BDF method.

To study the effect of various system parameters on the system response, we constructed a dimensionless parameter C_t that is obtained by dividing C by l_{10}, i.e., $C_t = EA/(ml_{10}\Omega^2)$. At first, we study the effects of the initial spin rates β_0' on the system response (Figs. 2 and 3). We consider the system having equal satellite masses, i.e., $\mu_1 = \mu_2 = \mu_3 = \frac{1}{3}$. It is observed that when β_0' is taken as 0.5 the system becomes unstable as tethers get slacked. In fact, the similar results were obtained earlier by Tragesser.[22] However, when β_0' is 0.6, which is just above the critical value, i.e., $(\beta_0')_{\rm cr} = 0.58$, the response shows stable system motion. The further increase in β_0' results in the similar stable system response with the reduction in tether oscillations (Fig. 3). While the system is rotating, the variations in tether tensions as derived analytically match very well with the numerical simulation. The period of tether oscillations is found to be 180 deg. The changes in β_2 and β_3 follow the same trend as of β_1. The effects of the out-of-plane swing rates η_0' on the system response are shown in Fig. 4. It is observed that even in the presence of $\eta_0' = 0.01$ the system remains stable, and η_1 and η_2 responses remain bounded. However, if η_0' is taken very high in comparison to the in-plane swing rate β_0' of 0.6, say, 0.2, the tethers get slackened and the system can become unstable. In this situation, if initial spin rate β_0' is taken 0.7, then the system shows stable motion.

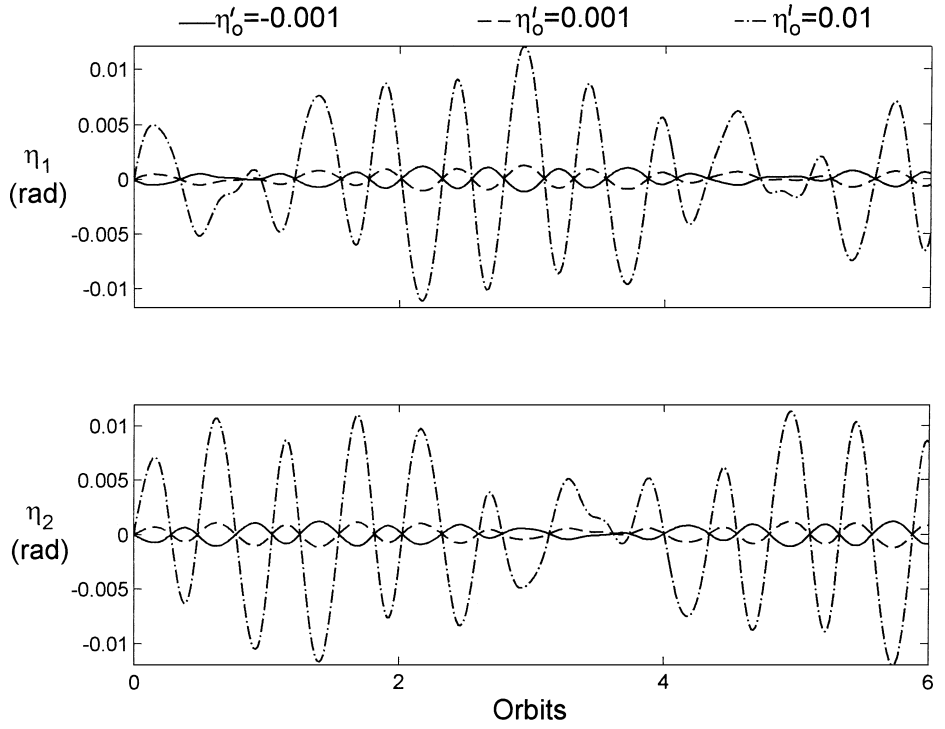

Fig. 4 Typical system response as affected by out-of-plane swing rates η_0': $e = 0$, $C_t = 10^5$, $l_{t0} = 1$ km, $\mu_1 = \mu_2 = \mu_3 = \frac{1}{3}$, and $\beta_0' = 0.6$.

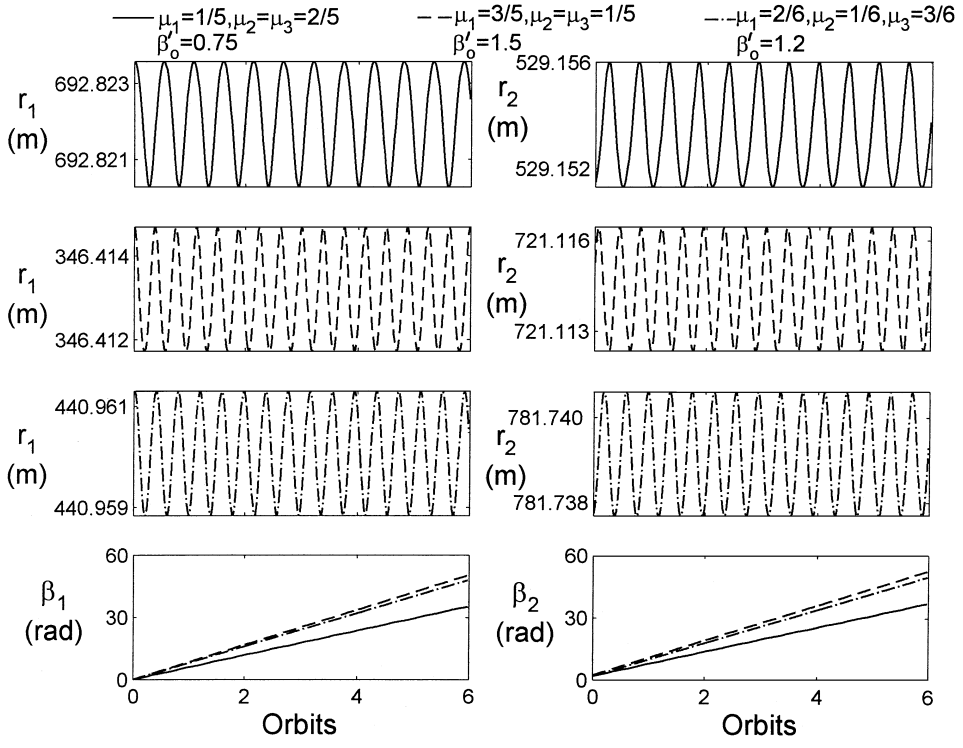

Fig. 5 Typical system response as affected by satellite mass ratios: $e = 0$, $C_t = 10^5$, $l_{t0} = 1$ km, and $\eta_0' = 0$.

Figure 5 shows the effects of the satellite mass ratios on the system response. We first consider the case when satellite 2 and satellite 3 have equal masses. When the satellite mass ratios are taken as $\mu_1 = \frac{1}{5}$, $\mu_2 = \mu_3 = \frac{2}{5}$, the critical vale of β_0' obtained analytically is $(\beta_0')_{\rm cr} = 0.73$ while $(\beta_0')_{\rm cr}$ for the case $\mu_1 = \frac{3}{5}$, $\mu_2 = \mu_3 = \frac{1}{5}$ is 1.35. For the case when all satellite have different masses (i.e., $\mu_1 = \frac{2}{6}$, $\mu_2 = \frac{1}{6}$, $\mu_3 = \frac{3}{6}$), we assume the two tether lengths (i.e., $l_{10,e} = l_{20,e} = l_{r0} = 1$ km) and obtain the third tether length $l_{30,e}$ using the relation (43). In this case, we get $(\beta_0')_{\rm cr}$ as 1. The system shows stable response for all cases considered as the spin rate β_0' being taken is above the critical value.

The effects of tether lengths on the system response are shown in Fig. 6. With the increase in tether lengths from 500 m to 10 km, the system response remains almost unaffected except increase in the tether strains ε_1, ε_2, and ε_3 as the tether tension increases with the increase in the tether length. The tether deployment and retrieval have significant effects on the system response. In the case of deployment, Fig. 7a shows the stable system motion while the tether length is

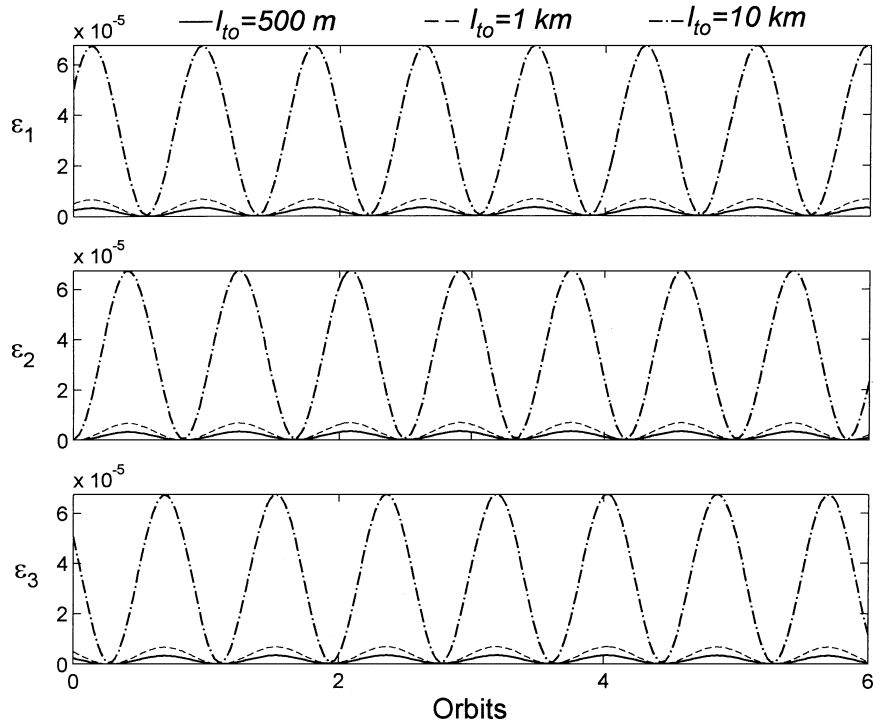

Fig. 6 Effects of tether lengths on system response: $e = 0$, $C = 10^8$ m, $\mu_1 = \mu_2 = \mu_3 = \frac{1}{3}$, $\beta_0' = 0.6$, and $\eta_0' = 0$.

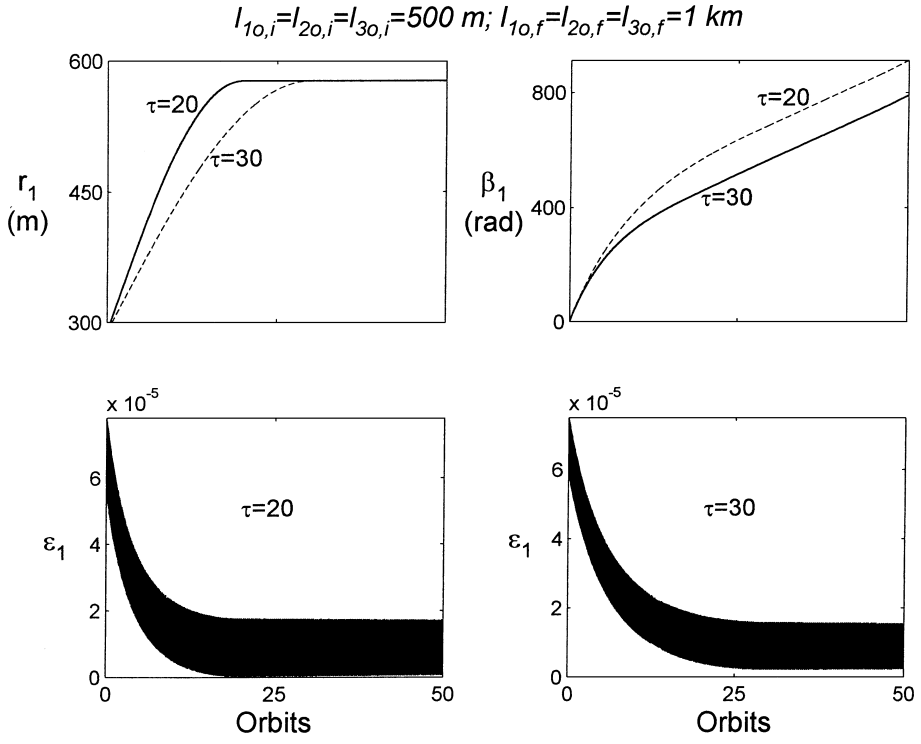

Fig. 7a Effect of tether deployment on system response: $e = 0$, $C = 10^8$ m, $\mu_1 = \mu_2 = \mu_3 = \frac{1}{3}$, $\beta_0' = 10$, and $\eta_0' = 0$.

increased from 500 m to 1 km and the initial spin rate β_0' taken as 10 that is above the critical spin rate of 5.32 as dictated by the condition (64). The r_i and β_i $(i = 2, 3)$ follow the same trend as of r_1 and β_1, respectively. The tether tensions decrease as the deployment proceeds. The tether strains ε_2 and ε_3 behave similarly as the tether strain ε_1 does. It is observed that the longitudinal frequency decreases from 1375 cycles per orbit for the initial tether length of 500 m to 950 cycles per orbit for the final tether length of 1 km (Fig. 7b). If the deployment rate is fast even though the spin rate is above the critical limit, there is a possibility of a tether getting slacked and it has been observed that if any one of the tethers gets slacked, even though the system is stable momentarily, it becomes unstable during long simulation time. With the high τ, the tether oscillations after the completion of deployment decrease, as expected. In the case of tether retrieval (Figs. 8a and 8b), the tether tensions increase with the retrieval as the spin rate increases, and thus the tethers never get slacked except the situation when the retrieval rate is fast. The longitudinal frequency shows the reverse trend from the tether deployment case

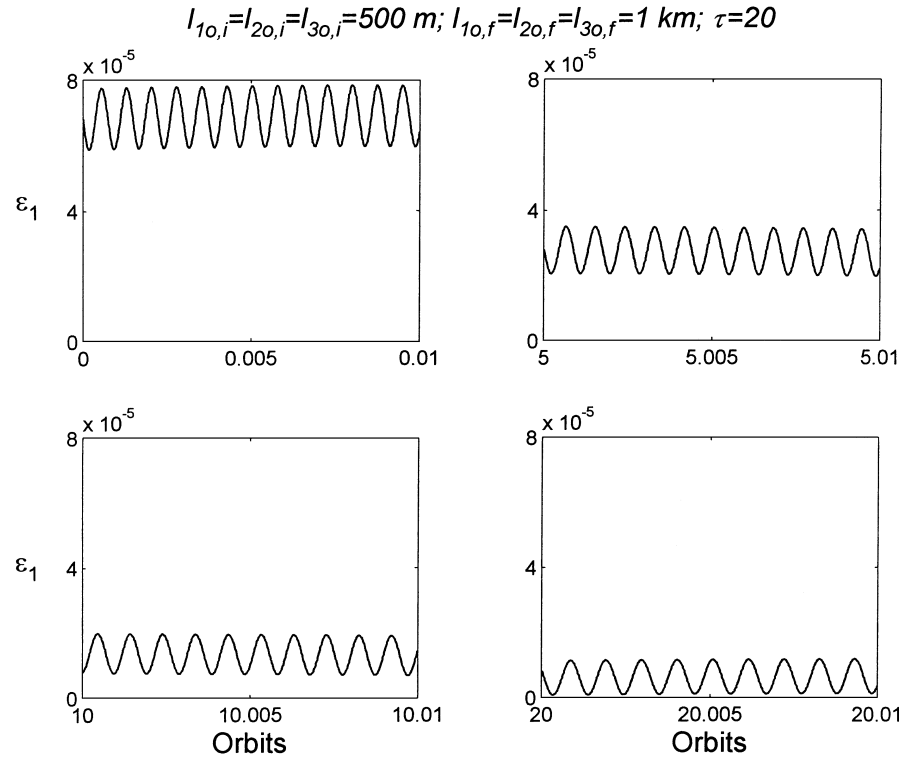

Fig. 7b Variation of tether strain during different stages of deployment: $e = 0$, $C = 10^8$ m, $\mu_1 = \mu_2 = \mu_3 = \frac{1}{3}$, $\beta_0' = 10$, and $\eta_0' = 0$.

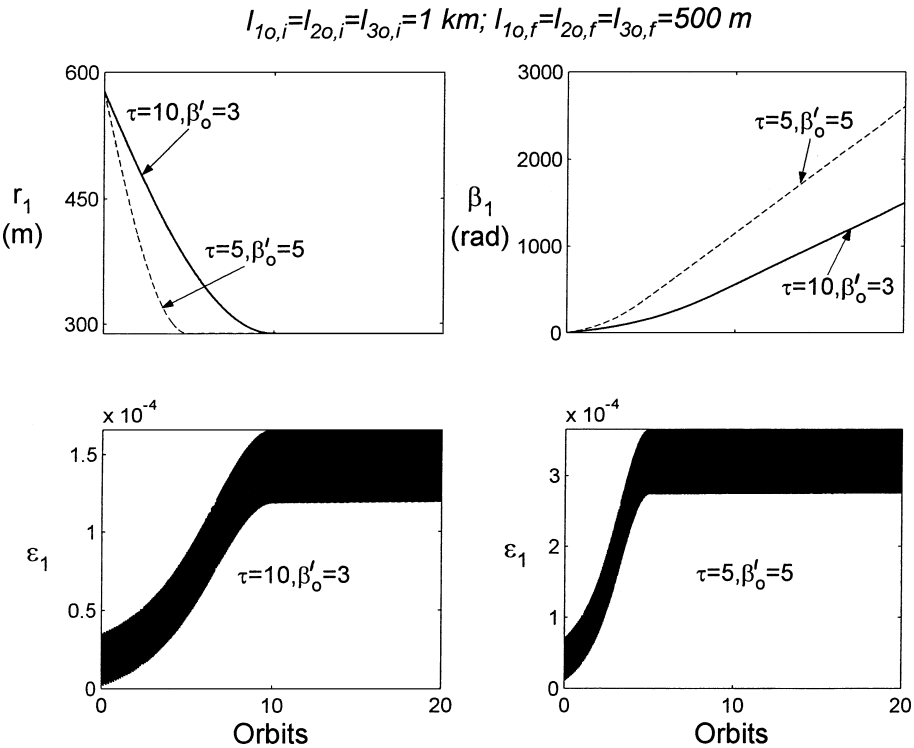

Fig. 8a Effect of tether retrieval on system response: $e = 0$, $C = 10^8$ m, $\mu_1 = \mu_2 = \mu_3 = \frac{1}{3}$, and $\eta_0' = 0$.

with an increase in oscillations from 950 cycles per orbit for the initial tether length of 1 km to 1375 cycles per orbit for the final tether length of 500 m (Fig. 8b). With the higher value of β_0', the tether retrieval can be accomplished in shorter duration. It is important to observe that the tether retrieval can be performed in shorter duration with the slower spin rate in comparison to the tether deployment.

The parameter C_t signifies tether rigidity and has a significant effect on the system response (Fig. 9). As C_t increases, the amplitudes of tether oscillations decrease and vice versa. In fact, the increase of C_t results in the increase of tether rigidity, and thereby the amplitudes of tether oscillations decrease and the system shows stable response. The critical or minimum value of C_t for the system steady-spin motion is obtained using Eq. (34) as 0.67. It has been observed that when C_t is below 5 the response starts with large tether oscillations, and finally the system becomes unstable.

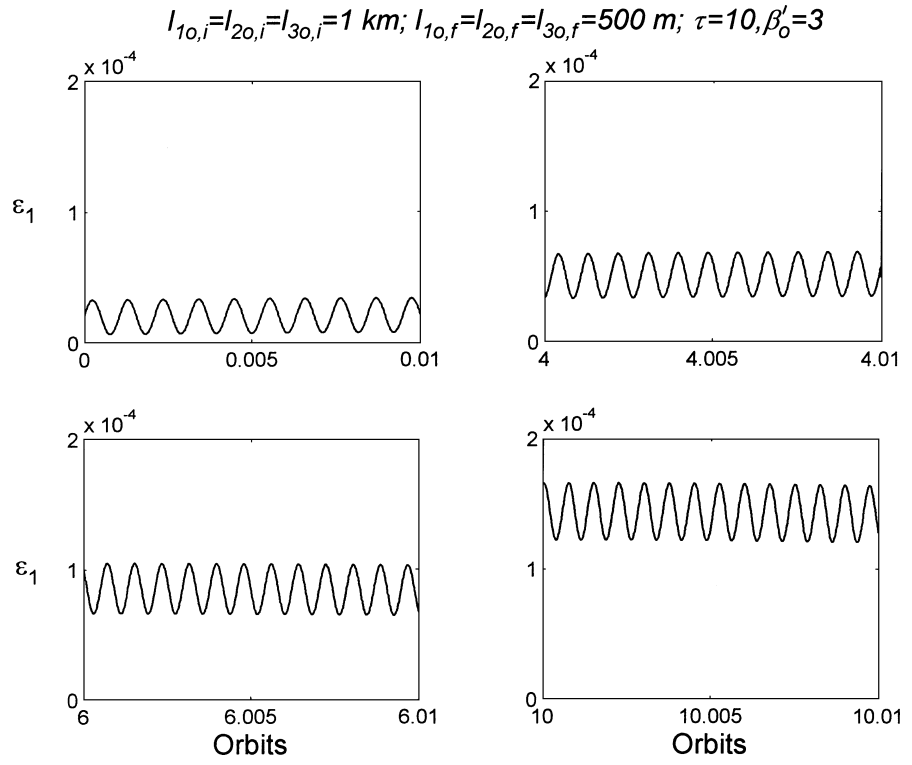

Fig. 8b Variation of tether strain during different stages of retrieval: $e=0$, $C=10^8$ m, $\mu_1=\mu_2=\mu_3=\frac{1}{3}$, $\eta'_0=0$.

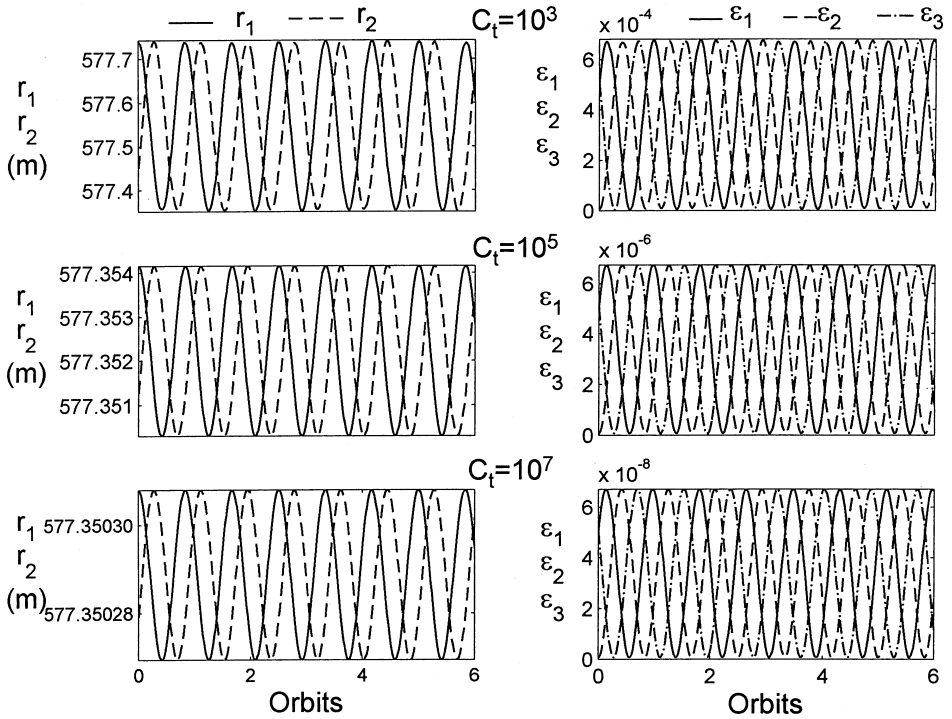

Fig. 9 Typical system response as affected by parameter C_t: $e=0$, $\mu_1=\mu_2=\mu_3=\frac{1}{3}$, $l_{t0}=1$ km, $\beta'_0=0.6$, and $\eta'_0=0$.

Next, we observe that even with eccentricity as high as 0.001 the system remains stable (Fig. 10). The r_1, r_2, β_1, β_2, ε_1, ε_2, and ε_3 remain almost unaffected with the changes in eccentricity from $e=0$ to 0.001. But r'_1, r'_2, β'_1, and β'_2 experience changes over an orbital period. In the case of eccentricity less than 0.0001, r'_1, r'_2, β'_1, and β'_2 change slightly compared to the situation when the system is moving in the circular orbit. With the orbital eccentricity of 0.0001, the oscillations of β'_1 and β'_2 coincide with the orbital period. Initially, β'_1 and β'_2 rise, and their values reach the highest at the apogee and then decrease and reach the lowest at the perigee. The reason for this behavior can be attributed to the term containing $2e\sin\theta$ in the equations of motion [Eq. (12)] for β_1 and β_2. The $2e\sin\theta$ term grows as the true anomaly θ changes from 0 to 180 deg and diminishes while θ changes from 180 to 360 deg. This term, in fact, dominates the case when the orbital eccentricity is higher than 0.0001. In the case of high eccentricity, say, $e=0.2$, the system exhibits response

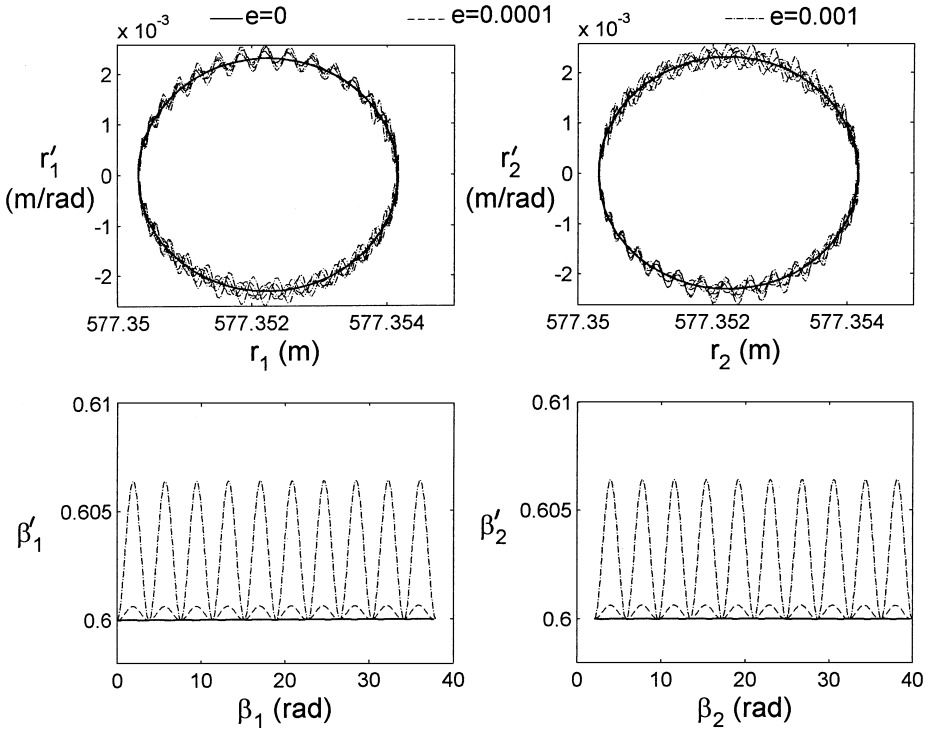

Fig. 10 Typical system response as affected by orbital eccentricity: $C_t = 10^5$, $\mu_1 = \mu_2 = \mu_3 = \frac{1}{3}$, $l_{t0} = 1$ km, $\beta'_0 = 0.6$, and $\eta'_0 = 0$.

with high amplitudes and fast oscillations of r'_1 and r'_2 and tether strains. Additionally, the amplitudes of β'_1 and β'_2 increase without change in their periods of oscillations, resulting in fast system spin rate and slackening of tethers.

Conclusions

An analysis of rotating formation flying of three satellites using flexible tethers is presented in this paper. An equilibrium analysis undertaken here leads to several inequality constraints on system parameters. These facilitate a judicious choice of various system parameters for an inherently stable design. Results of numerical integrations of the governing nonlinear equations of motion along with the equilibrium conditions indicate that the proposed concept is feasible. The effects of various system parameters and tether deployment/retrieval on the system response have been investigated. It is found that it is possible to have formation flying of satellites in the orbital plane if the system spin rate is greater than the critical value of 0.58 times the orbital rate. Thus, the present analysis is an attempt towards understanding the dynamics and control aspects of formation flying of satellites and can serve as a basis to solve problems of formation flying in any arbitrary plane as well as the reorientation of the direction of the formation that would be considered in future work.

Acknowledgment

The authors acknowledge the support for this study provided by the Japan Society for the Promotion of Science.

References

[1]Vassar, R. H., and Sherwood, R. B., "Formationkeeping for a Pair of Satellite in a Circular Orbit," *Journal of Guidance, Control, and Dynamics*, Vol. 8, No. 2, 1985, pp. 235–242.

[2]Wang, P. K. C., and Hadaegh, F. Y., "Coordination and Control of Multiple Microspacecraft Moving in Formation," *Journal of Astronautical Sciences*, Vol. 44, No. 3, 1996, pp. 315–355.

[3]de Queiroz, M. S., Kapila, V., and Yan, Q., "Adaptive Nonlinear Control of Multiple Spacecraft Formation Flying," *Journal of Guidance, Control, and Dynamics*, Vol. 23, No. 3, 2000, pp. 385–390.

[4]Kapila, V., Sparks, A. G., Buffington, J. M., and Yan, Q., "Spacecraft Formation Flying: Dynamics and Control," *Journal of Guidance, Control, and Dynamics*, Vol. 23, No. 3, 2000, pp. 561–564.

[5]Kang, W., Sparks, A. G., Banda, S., "Coordinated Control of Multisatellite Systems," *Journal of Guidance, Control, and Dynamics*, Vol. 24, No. 2, 2001, pp. 360–368.

[6]Sabol, C., Burns, R., and McLaughlin, C. A., "Satellite Formation Flying Design and Evolution," *Journal of Spacecraft and Rockets*, Vol. 38, No. 2, 2001, pp. 270–277.

[7]Vadali, S., Schaub, H., and Alfriend, K. T., "Initial Conditions and Fuel-Optimal Control for Formation Flying of Satellites," AIAA Paper 99-4265, Aug. 1999.

[8]Inalhan, G., and How, J. P., "Relative Dynamics and Control of Spacecraft Formations in Eccentric Orbits," *Journal of Guidance, Control, and Dynamics*, Vol. 25, No. 1, 2002, pp. 48–59.

[9]Tillerson, M., and How, J. P., "Formation Flying Control in Eccentric Orbits," AIAA Paper 2001-4092, Aug. 2001.

[10]Misra, A. K., and Modi, V. J., "A Survey on the Dynamics and Control of Tethered Satellite Systems," *Advances in the Astronautical Sciences*, Vol. 62, 1986, pp. 667–719.

[11]Beletsky, V. V., and Levin, E. M., *Dynamics of Space Tether Systems, Advances in the Astronautical Sciences*, Vol. 83, 1993.

[12]Cosmo, M. L., and Lorenzini, E. C., *Tethers in Space Handbook*, 3rd ed., NASA Marshall Space Flight Center, Huntsville, AL, Dec. 1997.

[13]Quadrelli, M. B., and Lorenzini, E. C., "Dynamics and Stability of a Tethered Centrifuge in Low Earth Orbit," *Journal of the Astronautical Sciences*, Vol. 40, No. 1, 1992, pp. 3–25.

[14]Terrestrial Planet Finder Science Working Group, *Terrestrial Planet Finder*, edited by C. A. Beichman, N. J. Woolf, and C. A. Lindensmith, NASA Jet Propulsion Lab., California Inst. of Technology, JPL Publ. 99-003, Pasadena, CA, May 1999.

[15]DeCou, A. B., "Tether Static Shape for Rotating Multimass, Multitether, Spacecraft for 'Triangle' Michelson Interferometer," *Journal of Guidance, Control, and Dynamics*, Vol. 12, No. 2, 1989, pp. 273–275.

[16]DeCou, A. B., "Gravity Gradient Disturbances on Rotating Tethered Systems in Circular Orbit," *Proceedings of 3rd International Conference on Tethers in Space—Towards Flight*, AIAA, Washington, DC, 1989, pp. 343–351.

[17]DeCou, A. B, "Attitude and Tether Vibration Control in Spinning Tethered Triangles for Orbiting Interferometry," *Journal of the Astronautical Sciences*, Vol. 41, No. 3, 1993, pp. 373–398.

[18]Quinn, D. A., and Folta, D. C., "A Tether Formation Flying Concept for the SPECS Mission," *Advances in the Astronautical Sciences*, Vol. 104, 2000, pp. 183–196.

[19]Quadrelli, M. B., "Modeling and Dynamics Analysis of Tethered Formations for Space Interferometry," *Advances in the Astronautical Sciences*, Vol. 108, Pt. 2, 2001, pp. 1259–1278.

[20]Bombardelli, C., Lorenzini, E. C., and Quadrelli, M. B., "Pointing Dynamics of Tether-Controlled Formation Flying for Space Interferometry," *Advances in the Astronautical Sciences*, Vol. 109, Pt. 2, 2001, pp. 1539–1552.

[21]Misra, A. K., Bellerose, J., and Modi, V. J., "Dynamics of a Tethered System near the Earth-Moon Lagrangian Points," *Advances in the Astronautical Sciences*, Vol. 109, Pt. 1, 2001, pp. 415–435.

[22]Tragesser, S. G., "Formation Flying with Tethered Spacecraft," American Astronautical Society, Paper 2000-4133, Aug. 2000.

[23]Williams, T., and Moore, K., "Dynamics of Tethered Satellite Formations," *Advances in the Astronautical Sciences*, Vol. 112, Pt. 2, 2002, pp. 1219–1235.

[24]Tragesser, S. G., and Tuncay, A., "Orbital Design of Earth-Oriented Tethered Satellite Formations," American Astronautical Society, Paper 2002-4641, Aug. 2002.

[25]Mori, O., and Matunga, S., "Coordinated Control of Tethered Satellite Cluster Systems," AIAA Paper 2001-4392, Aug. 2001.

C. McLaughlin
Associate Editor